Global NEST Journal, Vol 26, No 10, 06047

Adsorption of carotenoids, chloride, and sulfate from annatto dye agro-industrial effluent

Bárbara Fernanda Rosa[1], Rodrigo Fernando dos Santos Salazar[2], Mateus Nordi Esperança[1] and André Luís de Castro Peixoto[1]*
[1]Research Group on Process Chemistry (ProChem), Federal Institute of Education, Science and Technology of São Paulo (IFSP), Capivari Campus, Capivari, São Paulo, CEP 13365-010, Brazil.
[2]Passo Fundo University, BR 285 km 292,7, Campus I, Passo Fundo, Rio Grande do Sul, CEP 99052-900, Brazil.
Received: 11/04/2024, Accepted: 18/08/2024, Available online: 08/10/2024
*to whom all correspondence should be addressed: e-mail: alcpeixoto@ifsp.edu.br
https://doi.org/10.30955/gnj.06047

Graphical abstract

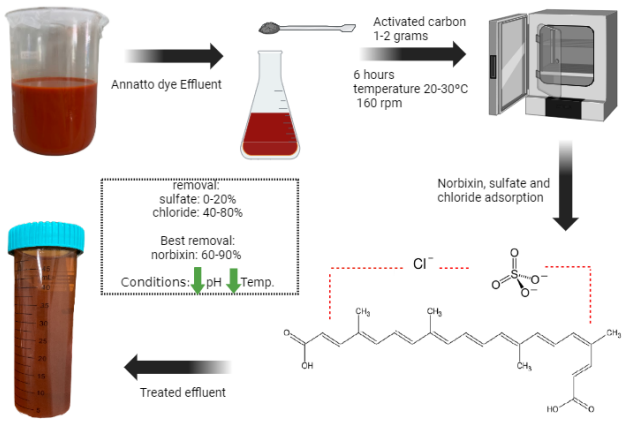

Abstract

Natural dyes, such as annatto, are widely used in the food and pharmaceutical industries. However, the effluents from annatto dye production pose environmental challenges due to the presence of residual dye components, organic matter, and dissolved inorganic species (chloride and sulfate). This study, the first attempt in the literature to deal with real annatto dye effluent, aimed to evaluate the use of activated carbon for the removal of carotenoids (norbixin), chloride, and sulfate. A 2^3 full-factorial design was employed to optimize the adsorption process parameters (temperature, pH, and adsorbent mass). The results showed that up to 90% of carotenoids and chloride could be removed under optimized conditions (low temperature and pH). Sulfate removal was more strongly influenced by the pH of the medium, with a maximum removal of 53%. The adsorption process was well-described by empirical models, though traditional isotherm models did not adequately represent the experimental data. Hypotheses that support isotherm models such as pore homogeneity, monolayer formation, constant internal diffusion were not satisfied. This study demonstrates the potential of activated carbon adsorption as a feasible method for treating food industry effluents containing high loads of carotenoids and inorganic salts.

Keywords: adsorption; annatto; natural dyes; bixin; norbixin; carotenoids; sulfate; chloride; agricultural wastewater; activated carbon.

1. Introduction

Also known as E160b, the Annatto dye is a natural food coloring obtained from the seeds of the achiote tree (*Bixa orellana*). The dye is derived from the reddish-orange outer coating of seeds and is commonly used in the food industry to impart a yellow to orange color to various food products and for pharmacological applications (Coelho Dos Santos *et al.* 2022; Hirko & Getu, 2022; Kapoor & Ramamoorthy, 2021; Samanta & Singhee, 2023).

Annatto dye is primarily produced in tropical regions, particularly South America. The achiote tree seeds is harvested, dried, and processed to extract the dye. Extraction methods include steeping the seeds in water or oil, followed by filtration to obtain concentrated annatto dye (Samanta & Singhee, 2023). In relation to its composition, those main coloring components found in annatto dye are bixin, norbixin, minor carotenoids and fatty acids (Hirko & Getu, 2022). Bixin is the major pigment present in annatto dye, accounting for approximately 70-80% of the color content. It is an apocarotenoid belonging to the carotenoid family. Bixin is responsible for the intense reddish-orange color of the annatto dye. Norbixin is a partially degraded form of bixin and accounts for the remaining 20-30% of the color content of annatto dye. It is also an apocarotenoid that contributes to the overall shade color, ranging from yellow to orange. In addition to bixin and norbixin, annatto dye may contain minor carotenoids such as cis-bixin and dihydrobixin in smaller quantities. These minor carotenoids contribute to the overall color profile of the annatto dye. Annatto seeds also contain fatty acids that are responsible for the lipophilic nature of the dye. Fatty acids act as carriers for color pigments and aid their extraction (Coelho Dos Santos *et al.* 2022; Hirko & Getu, 2022; Samanta & Singhee, 2023).

In the annatto dye extraction process, the resultant wastewater is characterized by the presence of residual dye components, organic matter, suspended solids, and a spectrum of dissolved entities including, but not limited to, carotenoids, chlorides, and sulfates. Notably, while annatto dye itself is devoid of significant concentrations of sulfate or chloride ions, these constituents are introduced into the wastewater through the utilization of water that inherently contains these ions during the dye extraction and production phases. This necessitates a nuanced understanding of the wastewater profile associated with annatto dye manufacturing, as elucidated in our analysis and corroborated by the literature (Boguniewicz-Zablocka *et al.* 2020; Hirko & Getu, 2022; Kapoor & Ramamoorthy, 2021).

A critical step in the annatto dye production process involves the precipitation of the dye mass, during which the introduction of chloride and sulfate ions is facilitated through the application of strong acids such as HCl and H_2SO_4. This stage represents a pivotal point of consideration for the subsequent treatment strategies deployed for sulfate and chloride remediation, which are contingent upon the specific wastewater composition, regulatory directives, and the presence of other co-contaminants.

Parallel to the issues posed by inorganic ions, the effluent streams from annatto dye processing and analogous sectors, notably within the food processing industry, are characterized by the presence of carotenoids. These compounds, despite their natural origin, pose environmental challenges when present in effluents. Addressing this, research endeavors have been directed towards the development of efficacious carotenoid adsorption techniques aimed at mitigating their environmental impact.

In response to the multifaceted challenges presented by annatto dye wastewater, a spectrum of treatment methodologies has been proposed, ranging from conventional sedimentation and filtration to advanced mass transfer-based processes such as adsorption and reverse osmosis. The selection of an appropriate treatment paradigm is intricately linked to local regulatory frameworks, the quality of treated water required, and the potential for discharge or reuse within specified applications.

The adsorption process, in particular, emerges as a versatile and highly adaptable solution for pollutant removal from wastewater, attributed to its simplicity, scalability, and compatibility with existing treatment infrastructures. Studies on carotenoid adsorption in liquid effluents are essential for developing sustainable and efficient strategies to mitigate their loss and environmental impact while harnessing their many potential benefits, such as development of eco-friendly and cost-effective adsorption processes for large-scale applications; understanding the adsorption behavior of carotenoids in complex matrices and real wastewater samples; integration of adsorption processes with emerging technologies for efficient carotenoid recovery; and assessment of the economic feasibility and life cycle analysis of carotenoid adsorption processes (Bouazizi *et al.* 2022; Gama *et al.* 2022; Kalra *et al.* 2021; Pavithra *et al.* 2019; Rathi & Kumar, 2021). Therefore, our objective was to study the adsorption removal of carotenoids (norbixin), chloride, and sulfate from the real effluent of the annatto dye food industry. As there have been no studies involving this effluent, we opted to use commercial activated carbon without any prior surface treatment. The effluent was applied without any prior treatment.

2. Materials and Methods

2.1. Reagents

Commercial activated carbon (*Dinâmica* Co.) was used in all the experiments. The activated carbon was pre-treated by washing with ultrapure water, followed by drying at a constant temperature of 70 °C until it reached a constant weight. Further technical and safety details regarding activated carbon can be found on the manufacturer's website. Additionally, details regarding the characterization of this material will be presented in section 2.5. Water used for the project was purified using a Milli-Q Direct 8 system. A 1.0 mol/L solution of KOH was utilized to adjust the pH of the experiments. KOH was purchased from *Ecibra Reagentes Analíticos*.

2.2. Adsorption Processes

Carotenoid adsorption was performed using a batch process. The agro-industrial effluent was used in its raw form (without dilution or previous physicochemical treatment), and 50.0 mL was used for all the experiments. Each experiment was conducted in a closed system using a glass bottle containing commercial activated carbon and the effluent. Commercially activated carbon was used without surface modification, that is, in how it was purchased. The mass of activated carbon was weighed using an analytical balance (WEBLABOR M254-Ai). Experiments were conducted for six hours at 160 rpm in an incubator (Lucadema LUCA-223) with orbital agitation and temperature control. The amount of adsorbent, temperature, and pH were determined using a 2-level full-factorial design. The pH of the experiments was adjusted with a 1.0 mol/L KOH solution because the original pH of the raw effluent was 1.9. Aliquots for chemical analyzes were taken at pre-defined time intervals: 0, 30, 60, 120, 360, 720 and 1440 minutes.

2.3. Experimental design and statistical analysis

A 2^3 full-factorial design was used to assess the effects of three independent variables on norbixin, chloride, and sulfate removal: temperature (T), adsorbent mass (m_{ads}), and pH. The experimental design comprised 11 runs: eight axial points, and three central points (to assess the error of the adsorption process). The independent variables were set at two levels and a central point as follows:

- Temperature = 20 °C (–1), 30 °C (0), and 40 °C (+1).
- pH = 2.50 (–1), 4.00 (0), and 5.5 (+1).
- Adsorbent mass = 2.0000 g (–1), 3.0000 g (0), and 4.0000 g (+1).

The STATISTICA 7.0 statistical software package was used to analyze the experimental data, generate analysis of variance (ANOVA) results, and plot response surfaces.

2.4. Chemical Analysis

2.4.1. Determination of Carotenoids

Norbixin analyses were performed using a Thermo Scientific Genesys 10-S double-beam spectrophotometer. The samples were diluted with a 0.5% m/v KOH solution and the absorbance was read at 453 nm. Glass cuvettes with a 1 cm optical path were used. A molar absorptivity of 2,850, as proposed by Reith and Gielen (Reith & Gielen, 1971), was considered for the analyses.

2.4.2. Determination of Sulfate

Sulfate analyses were performed using the turbidimetric method (*SW-846 Test Method 9038: Sulfate (Turbidimetric)*, 1986) by treating the acidified sample with barium chloride. The reaction of sulfate ions and barium chloride yielded a barium sulfate suspension. The applied method is suitable for the analysis of drinking water, surface water, and domestic and industrial effluents at 1–40 mg/L. Analyses were performed using test kits reagents HI38000-10 (Hanna Instruments). The barium sulfate suspensions were read using a benchtop photometer (model HI83300, Hanna Instruments).

2.4.3. Determination of chloride

Chloride analyses were performed by adapting the mercury(II) thiocyanate method (Florence & Farrar, 1971), in which the reaction of chloride and the reagent produces an orange-colored product in the sample. Thiocyanate ions (SCN^-) are liberated from mercuric thiocyanate through mercury sequestration by chloride ions to form unionized mercuric chloride. In the presence of ferric ions, the liberated SCN^- form is highly colored ferric thiocyanate at a concentration proportional to the initial chloride concentration. The applied method is appropriate for 0–20 mg/L, which fits analyses of drinking water, surface water, and domestic and industrial effluents. Analyses were performed using test kit reagents HI93753 A and B (Hanna Instruments). Ferric thiocyanate readings were obtained using a benchtop photometer model HI83300 (Hanna Instruments).

2.4.4. Total Organic Carbon (TOC) and Total Nitrogen (TN)

Total Organic Carbon (TOC) analyses (D19 Committee, n.d.-b) were performed according to the combustion catalytic oxidation method using a Shimadzu TOC-L apparatus. Total Nitrogen (TN) analyses (D19 Committee, n.d.-a) were performed using the chemiluminescence method with Shimadzu TNM-L equipment.

2.4.5. Multi-elemental characterization

An optical emission spectrometer with inductively coupled plasma optical emission spectrometry (ICP-OES, Perkin Elmer Avio 500) was used for multi-elemental characterization (Ba, Cd, Cr, Cu, and Pb) of the raw effluent. This equipment can use plasma in both axial and radial configurations. The effluent samples were digested using the nitric perchloric digestion method, as described by Salazar et al. (Salazar *et al.* 2011). The sample preparation method and analytical results were validated using reference material (RM) of agronomic residue from the *Instituto Agronômico de Campinas* (IAC-FM-2021 and IAC-CA-2021).

2.5. Activated carbon physico-chemical characterization

The specific surface area, particle size, pore volume and distribution were calculated and determined by $\mathbf{N_2}$ adsorption (77 K) (Micromeritics Gemini VII). The activated carbon samples were degassed at 300 °C for 16 h using a Micromeritics VacPrep 061 instrument.

The infrared spectra of the adsorbent samples were acquired using the potassium bromide pellet technique. The powder of each adsorbent was finely ground and combined with potassium bromide in a 1:100 ratio by weight. 0.1 g of the mixture was precisely measured and pressed into a pellet to obtain the infrared absorption spectra. The infrared spectra were measured from 4000 to 400 cm^{-1} (2.5 to 25 µm) at a resolution of 4 cm^{-1} per data point and 32 scans per sample using a Frontier FT-IR spectrometer from (PerkinElmer Inc., USA).

3. Results

3.1. Raw effluent characterization

Prior to the adsorption experiments, analyses were carried out to characterize the raw effluent, which consisted of a saline aqueous phase containing carotenoids as norbixinate and a solid phase in suspension composed of carotenoids in the liposoluble form known as bixin. Untreated wastewater had a conductivity of 15,204 ± 1,260 µS/cm (*n*= 10; mean ± standard deviation). The concentrations of total organic carbon (TOC) and total nitrogen (TN) were determined using three different raw industrial effluent samples. The mean TOC and TN values were 4,838 ± 158 mg/L and 314.7 ± 17.4 mg/L, respectively. An ICP-OES analysis was performed, resulting in the following concentrations: Cd 15.2 ± 1.0 µg/L, Pb: 7.7 ± 3.6 µg/L, Ba: 79.7 ± 1.2 µg/L, Cr: 49.6 ± 1.0 µg/L, and Cu: 0.144 ± 0.003 mg/L.

Photometric analyses were conducted to quantify carotenoids, chlorides, and sulfates in the annatto seed effluent before and after filtration. Carotenoid concentrations were expressed as norbixin equivalents, based on the Beer-Lambert law. In the crude, unfiltered effluent, norbixin concentration was measured as 0.0838 ± 0.0053 mol/L, equivalent to 31.88 ± 2.02 g/L (*n*=5 replicates). Filtration through quantitative filter paper significantly reduced soluble norbixin, with a post-filtration concentration of 0.01242 ± 0.0051 mol/L or 4.73 ± 1.94 g/L (*n*=5). Similarly, chloride levels decreased from 15.28 ± 0.69 g/L (*n*=5) in the crude effluent to 0.45 ± 0.11 g/L (*n*=5) following filtration. Sulfate was present at 10.78 ±0.49 g/L (*n*=5) before filtration and 9.96 ± 0.92 g/L (*n*=5) in the filtered effluent.

3.2. Activated carbon physico-chemical characterization

With an approximately 0.1 mg of sample, it was possible to calculate the specific surface area of the activated carbon used in this study. With five experimental points, a result of 411.6253 m^2/g was obtained, with an uncertainty of 3%.

Figure 1. shows the activated carbon functional groups responsible for the adsorption of carotenoids, chlorides, and sulfates.

Table 1. Full 2-level factorial experimental design. Independent variables: temperature (°C), activated carbon mass (g), and pH with real (uncoded) and coded values. Response (or dependent) variables: Carotenoids, sulfate, and chloride removal (%). Triplicate central-point condition.

Temperature (°C)	Adsorbent (g)	pH (-)	Carotenoids removal (%)	Sulfate removal (%)	Chloride removal (%)
20.0 (-1)	2.0000 (-1)	2.50 (-1)	90.67	15.59	97.79
40.0 (1)	2.0000 (-1)	2.50 (-1)	60.30	9.63	49.22
20.0 (-1)	4.0000(1)	2.50 (-1)	89.47	0.47	62.03
40.0 (1)	4.0000 (1)	2.50 (-1)	69.09	8.92	84.54
20.0 (-1)	2.0000 (-1)	5.50 (1)	90.22	53.00	67.32
40.0 (1)	2.0000 (-1)	5.50 (1)	86.92	7.98	41.50
20.0 (-1)	4.0000 (1)	5.50 (1)	82.34	14.55	84.54
40.0 (1)	4.0000 (1)	5.50 (1)	90.16	13.61	93.37
30.0 (0)	3.0000 (0)	4.00 (0)	83.60	20.18	70.86
30.0 (0)	3.0000 (0)	4.00 (0)	86.16	15.49	65.12
30.0 (0)	3.0000 (0)	4.00 (0)	85.41	22.06	69.53

Table 2. Chloride removal values reported for different effluents and adsorbents.

Reference	Adsorbent	Adsorbent dosage (g/L)	T (ºC)	pH (-)	Contact time (min)	Liquid phase	Chloride initial concentration (mg/L)	Removal (%)
Present study	Activated carbon	40-80	20-40	2.5-5.5	360	Annatto Dye Effluent	450	41-98
Dey et al. (2024)	Rice husk	0.005-0.025	-		120	Model effluent	1	5-20
	Parthenium							20-65
	Egg shell							12-32
	Rape straw							3-10
	Sawdust							8-25
	Parthenium	0.018-0.022	10-45	4-7.5	15-150	Model effluent	1	17-65
Moosaei *et al.* (2024)	AgMX [1]	0.2-2	-	-	1-17	Chloride solution	10-90	41.9-91.8
Sarani et al. (2024)	Grapheme oxide modified with $AgNO_3$	0.5-2.5	Room temperature	-	1-65	Chloride solution	10-90	34-99
Singh et al. (2024)	nFeO decorated wood biochar	-	Room temperature	6.5	-	Tannery effluent	470.4	68 [2]
	nFeO decorated wood biochar	-			-			90 [3]
Alexander Zengeya et al. (2024)	Mayenite-based Ca/Al oxides (CAO) [4]	10% [5]	-	12	120	Flue gas desulfurization (FGD) wastewater	4,437.5	4-72
		1-20% [5]		12	120			4-80
		10% [5]		8-12	120			43-68
		10% [5]		12	60-300			60-77

[1]Silver nanoparticles-modified Ti3C2 MXene nanocomposite.

[2]Continuous adsorption process. Independent parameters evaluated: feed flow rate (2.5 and 5mLmin− 1), and the height of the fixed bed of adsorbent (3.5 and 5.5 cm).

[3]Coupled coagulation-continuous adsorption process.

[4]Mayenite (Ca12Al14O33).

[5]Available data in %.

3.3. Adsorption process

To the best of our knowledge, no previous studies have evaluated annatto dye effluents. Then, conventional activated carbon was used in contact with the raw effluent and under constant agitation to remove carotenoids, chloride, and sulfate (Table 1). In the 6-hour

duration experiments, it was possible to obtain efficient carotenoid and chloride removal, with values ranging from 60 to 90% and from 41 to 98%, respectively (Table 1). In contrast, low sulfate removal was observed, with a maximum value of 53% (Table 1).

This temperature range (Table 1) adequately represents the ambient temperature in São Paulo (Brazil), where the annatto dye effluent was obtained. For industrial scale application it is unnecessary to heat or cool the effluent to be treated by adsorption.

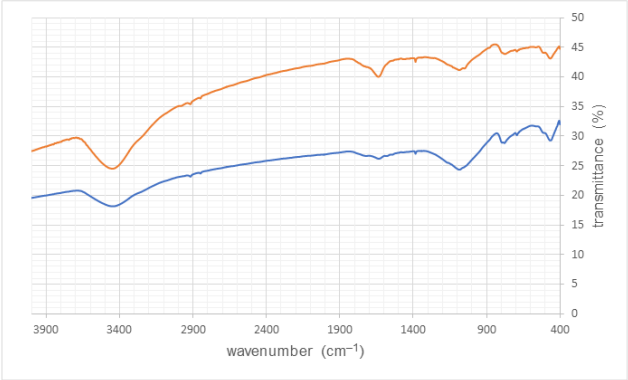

Figure 1. FTIR spectra of activated carbon before (blue line) and after (orange line) adsorption process.

The industry needs to lower the pH with sulfuric or hydrochloric acid to precipitate the mass of the natural dye. Industrial processes generate effluents with low pH values (pH <2) and high sulfate and chloride concentrations. We were consistent in presenting an adsorption study in this acidic pH range (Table 1).

Previously, we tested activated carbon in a smaller quantity (0.5 g), but the activated carbon, in this situation, removed carotenoids but did not remove the inorganics (data not shown). By increasing the amount of activated carbon (Table 1), we eliminated this barrier and allowed the adsorption of both carotenoids and inorganic ions, as presented in the Results section.

The elevated values for chloride removal exhibited in the present study are in agreement with previous adsorption tests performed with different adsorbents, as depicted in **Table 2**. It is important to highlight that most of the higher chloride removal data correspond to modified adsorbents, while commercial activated carbon was used in the present study.

3.3.1. Carotenoid removal

According to the central point in triplicate, the carotenoid removal process had an error of 1.5% (**Table 1**). An initial evaluation of the experimental data showed that the errors (residues) exhibited a normal distribution and random pattern and that there were no outliers (**Fig. S1; Supplementary Materials**). Therefore, the carotenoid adsorption process yielded good data quality.

Based on the results presented in **Table 1**, an ANOVA was conducted to assess the main effects and interactions (second-order) between the factors. According to the ANOVA results of the complete model (**Table S1a, Supplementary Material**), linear temperature, linear pH, interaction between temperature and pH, and interaction between adsorbent mass and temperature were statistically significant (95% confidence interval). Then, non-significant terms were removed from the model, and a new ANOVA was performed (**Table S1b, Supplementary Material**).

These results indicated that the carotenoid removal model proposed (**Eq. 1**) accurately specifies the relationship between the process parameters and response variable. Eq. (1) represents the regression fit model for carotenoid adsorption by activated carbon.

$$y_1 = 83.1 - 5.8Cx_1 + 5.0Cx_3 + 2.6Cx_1Cx_2 + 6.9Cx_1Cx_3 \quad R^2 = 0.96 \quad (1)$$

where y_1 represents norbixin removal by adsorption (%), and x_1, x_2 and x_3 represent the coded factors of temperature, adsorbent mass, and pH, respectively.

To evaluate the predictive capacity of the model (**Eq. 1**), a plot of the predicted *versus* experimental norbixin removal was constructed (**Fig. S2, Supplementary Material**), indicating that Eq. (1) can estimate norbixin removal with an error lower than 5%. These results and the R^2 value indicate that the model could be used to evaluate the effects of temperature and pH on norbixin removal, which was performed by building a contour plot (**Fig. 2**). Because the regression model for norbixin removal contained all parameters (temperature, adsorbent mass, and pH), a value of 2.000 g for adsorbent mass (coded value: $x_2 = -1$) was fixed to generate the contour plot.

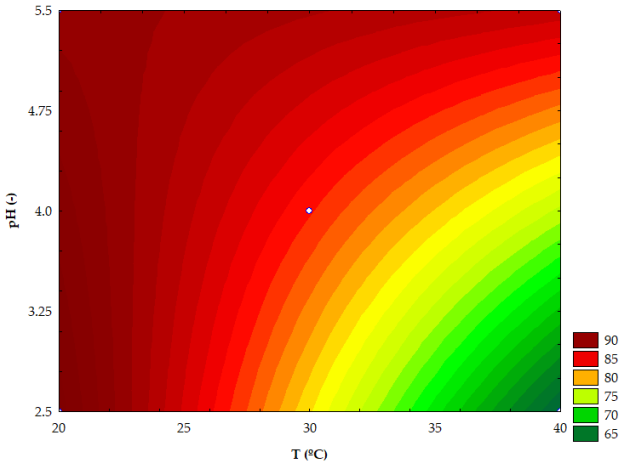

Figure 2. Contour plot of norbixin removal (%) as a function of pH and temperature (°C). (m_{ads} = 2.000g; x_2 = -1)

The contour plot of norbixin removal as a function of pH and temperature indicated that carotenoid removal was more efficient (higher than 90%, Fig. 2, red region) at low temperatures (below 25 °C) and low pH (below 3.25).

3.3.2. Chloride removal

According to the central point in triplicate, the chloride removal process had an error of 4.4% (**Table 1**). An initial evaluation of the experimental data showed that the errors (residues) exhibited a normal distribution and random pattern and that there were no outliers (**Fig. S3; Supplementary Materials**). Therefore, there was an

indication of the good quality of the data shown for the chloride adsorption process.

Based on the results presented in **Table 1**, an ANOVA was conducted to assess the main effects and interactions (second-order) between the factors. According to the ANOVA results of the complete model (**Table S2a, Supplementary material**), only the linear adsorbent mass, interaction between temperature and adsorbent mass, and interaction between adsorbent mass and pH were statistically significant (95% confidence interval). Linear temperature and pH factors were not statistically significant. Then, non-significant terms were removed from the model, and a new ANOVA was performed (**Table S2b, Supplementary Material**).

These results indicate that the proposed chloride removal model (**Eq. 2**) accurately specifies the relationship between the process parameters and the response variable. Eq. (2) represents the regression fit model for chloride adsorption by activated carbon.

$$y_2 = 71.4 + 8.6Cx_2 + 13.2Cx_1Cx_2 + 8.7Cx_2Cx_3 \quad R^2 = 0.85 \qquad (2)$$

where y_2 represents chloride removal by adsorption (%), and x_1, x_2, x_3 represent the coded factors of temperature, adsorbent mass, and pH, respectively.

To evaluate the predictive capacity of the model (**Eq. 2**), a plot of the predicted *versus* the experimental chloride removal was constructed (**Fig. S4, Supplementary Material**), indicating that Eq. (2) was able to estimate the chloride removal with an error lower than 10%. These results and the R^2 value indicate that the model could be used to evaluate the effect of the process parameters on chloride removal, which was performed by building a contour plot (**Fig. 3**). Because the regression model for chloride removal contained all parameters (temperature, adsorbent mass, and pH), a value of 2.000 g for adsorbent mass (coded value: x_2 = −1) was fixed to generate the contour plot.

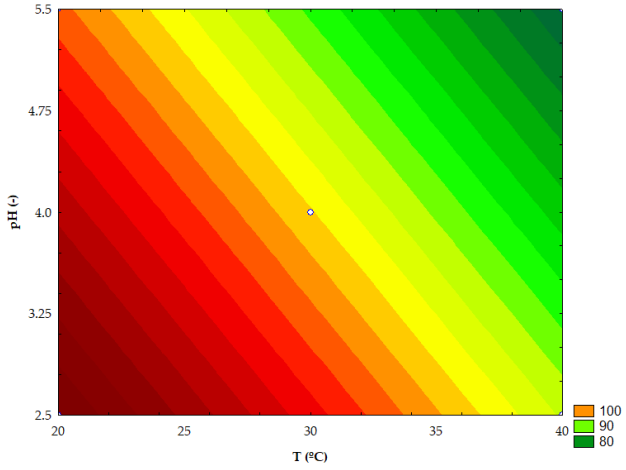

Figure 3. Contour plot of chloride removal (%) as a function of pH and temperature (°C). (m_{ads} = 2.000g; x_2 = -1)

The contour plot of chloride removal as a function of pH and temperature indicates that chloride removal was more efficient (Fig. 3, red region) at low temperatures and low pH.

3.3.3. Sulphate removal

The adsorption process promoted low sulfate removal, achieving a maximum value of 53% (**Table 1**). This performance was obtained at a low temperature (20 °C) and adsorbent mass (2.0000 g) associated with a high pH (5.50). In general, sulfate removal increased according to the following equation:

Decrease in temperature

Decrease in adsorbent mass

An increase on pH.

Despite this general visualization, ANOVA did not result in a model that allowed the evaluation of the effects of independent variables on sulfate removal with statistical confidence.

4. Discussion

4.1. Context of norbixin production

To extract alkaline solutions for norbixinate production, annatto seeds were placed in an extractor containing alkaline solutions of KOH or NaOH at concentrations close to 3% w/v, in a ratio of one-part seeds to two parts alkaline solution. The solution was then agitated to extract pigments from annatto grains. The grains were then separated, and a new extraction step was performed. The process was repeated to obtain > 90% extraction of the pigments (Carvalho, 2020).

Acidification of the annatto alkaline extract transforms norbixinate into norbixin. The pigment precipitated by acidification was then separated by filtration. This industrial norbixin production process uses strong acids (sulfuric or hydrochloric acid). The amount of acid added reduced the pH of the extract to values below 3. Thus, one of the biggest problems with this process is the need to treat the effluent with a high load of sulfate or chloride ions. Each ton of processed seeds can generate up to 2.5 m^3 of effluent with such characteristics (Carvalho, 2020).

4.2. Effluent characterization

The raw effluent exhibited a high conductivity of 15,204 ± 1,260 µS/cm (*n*= 10; mean ± standard deviation). Some of the observed effluent conductivity can be attributed to the salt forms of the extracted carotenoids such as norbixinate salts. Our analyses identified multiple mineral elements, including Ca, K, Cd, Pb, Ba, Cr, and Cu, in the annatto effluent. Furthermore, the effluent contained high residual sulfate and chloride levels from the acid treatment, which precipitated norbixin from the alkaline annatto extract. The norbixin pigment contributes to useful colorant properties, salts, heavy metals, and excess acidity, which introduce environmental concerns for effluent disposal. Further processing to remove extraneous components is required to improve the purity and safety.

Approximately 85% of the total carotenoid content in the industrial annatto processing effluent was present as particulate matter, while 15% remained dissolved. The

exceptionally high carotenoid concentrations, exceeding 30 g/L when expressed as norbixin equivalents, imply industrial inefficiency and waste of valuable pigments during commercial annatto seed processing. Only the dissolved carotenoid fraction was evaluated in the adsorption experiments to avoid interference from light-absorbing activated carbon fines during the spectrophotometric quantification of carotenoids. The samples were filtered post-treatment to remove residual carbon prior to the analysis.

Chloride and sulfate analyses indicated an effluent with the potential to cause salinization of drinking water sources, and implications for soil fertility and toxicity to aquatic ecosystems. The protein composition must be considered for high total nitrogen content in the effluent (315 mg/L). Annatto seeds are rich in protein. According to Carvalho (Carvalho, 2020), annatto seeds contain >10% protein in their composition. For high total organic carbon (TOC) content, the raw material contains 70% carbohydrates, >12% fiber and oils, in addition to carotenoids.

Only the dissolved chloride fraction was considered for the adsorption calculations. The presence of particulate matter, such as activated carbon, interferes with spectrophotometric analyses. However, for sulfate, there was no statistical difference between the dissolved and total fractions.

Valério et al. (Valério *et al.* 2015) researched the nutritional content of annatto seed residue, which involved the examination of essential amino acids, anti-nutritional factors, protein quality, and minerals. Copper, zinc, manganese, calcium, iron, and magnesium were analyzed using flame atomic absorption spectrometry, whereas calcium was measured using a flame photometer. Among the minerals found in annatto seeds, sodium (35.61 mg/g) and potassium (70.77 mg/g) showed the highest concentrations, followed by manganese (0.25 mg/g), calcium (0.11 mg/g), and copper, iron, and magnesium (0.03 mg/g).

Carvalho (Carvalho, 2020) reported on the composition of annatto seeds. Among the evaluated minerals, phosphorus (305 mg/100 g), calcium (237 mg/100 g), magnesium (270 mg/100 g), iron (2.40 mg/100 g), manganese (1.87 mg/100 g), zinc (0.49 mg/100 g), and sodium (0.90 mg/100 g) stood out among the evaluated minerals. Therefore, it is possible to observe that the raw material used by the annatto industry presents high levels of minerals, which justifies the high levels of conductivity and the metals quantified in this study.

4.3. Carotenoids removal

Carotenoids in industrial effluents can cause severe environmental damage if discharged without appropriate treatment. These compounds stimulate the consumption of dissolved oxygen, promote eutrophication, and negatively alter the natural color of water bodies. These three forms of impacts compromise ecological balance and water quality, as extensively documented in the literature. Therefore, the food industry must adopt effective technologies to remove residual carotenoids prior to the final discharge of their effluents. In addition to tertiary treatment (e.g., adsorption) and advanced oxidation processes, source minimization through good manufacturing practices can help mitigate this environmental problem. The first principle of Green Chemistry is that it is cheaper to avoid waste generation than to treat it after its production. Owing to the high levels of TOC, TN, and carotenoids dissolved in water, there is room for the industry to optimize the carotenoid extraction process from annatto seeds. In addition to noticeable production gains, optimizing the extraction process generates effluent with a lower treatment cost.

Owing to its complexity, the effluent studied here probably requires multiple processes for proper treatment and subsequent discharge into water bodies. However, activated carbon has been proven capable of removing carotenoids present in the effluent. Activated carbon with a high specific surface area and the functional groups presented in **Figure 1 (and Section 4.6)** can remove >90% of carotenoids through physisorption mechanisms. The physisorption mechanism is demonstrated by the increase in efficiency with decreasing process temperature (Eq. 1). Adsorption occurs through weak interactions between carotenoid molecules and functional groups such as van der Waals forces and hydrogen bonds. The lower the temperature, the lower the kinetic energy of the carotenoid molecules, which provides greater surface adhesion of the adsorbate to the adsorbent.

Pohndorf et al. (Pohndorf *et al.* 2016) investigated carotenoids and chlorophylls' adsorption kinetics, equilibrium, and thermodynamics during rice bran oil bleaching with activated earth. The adsorption process was carried out in batch mode, with a fixed amount of rice bran oil (40 g) and varying amounts of the activated earth adsorbent (from 0.5 to 2.5% w/w) and temperature (from 100 to 120 °C). The kinetic results showed that equilibrium was reached after approximately 45 min. The authors performed the experiments for 60 min to ensure that equilibrium was achieved. Carotenoid adsorption is spontaneous, endothermic, and chemisorption controlled. Higher temperatures and adsorbent doses increased the adsorption capacity, indicating chemisorption. Higher doses of activated earth lead to increased carotenoid adsorption capacity. At 120°C, the adsorption capacity increases from approximately 600 mg/kg at 0.5% to over 1000 mg/kg at 2.5%.

Li et al. (Z.-C. Li *et al.* 2023) studied the preparation of lignin-based covalent organic polymers (LIGOPD-COPs) and their application for removing carotenoids from vegetable extracts as a sample pretreatment for food safety analysis. The polymers had a porous structure and a moderate surface area. The LIGOPD-COPs prepared with 0.05% paraformaldehyde had a Brunauer-Emmett-Teller (BET) surface area of 30.87 m^2/g, whereas those prepared without paraformaldehyde had a lower surface area of 15.20 m^2/g. The optimal conditions for removing carotenoids from spinach extract were 1:1 water/acetonitrile ratio, 8 mg/L polymer dose, and 15 min equilibrium time. Under these conditions, 98% of the

carotenoids could be removed. They reported an adsorption capacity of 26.65 mg/g.

Shanshan et al. (Sun *et al.* 2016) reported synthesizing and characterizing a modified magnesium silicate material and its application as an adsorbent for β-carotene removal from hexane. Modified magnesium silicate was prepared hydrothermally using sodium silicate, magnesium nitrate, and aluminum sulfate. It exhibited a high specific surface area of 536.8 m^2/g. The material exhibited excellent adsorption capacity for β-carotene with a maximum value of 364.96 mg/g, much higher than standard magnesium silicate (71.74 mg/g). These results suggest that the material can be an effective adsorbent for carotenoid separation from organic solvents and oil decolorization.

Other studies (Igansi *et al.* 2019; Lau *et al.* 2019; Strieder *et al.* 2017) within the food industry have involved the adsorption of carotenoids. However, it is not possible to directly compare the literature results with those of our work. To the best of our knowledge, no studies have been conducted on wastewater treatment using carotenoids.

4.4. Chloride removal

Chloride contamination of water resources has become a pressing environmental concern because of the high solubility and persistence of chloride ions. The removal of chloride from industrial and municipal wastewater remains an unresolved technological hurdle. Elevated chloride concentrations have numerous detrimental effects, including pipeline corrosion (Guo *et al.* 2022), salinization of potable water supplies and fertile soils (Zhang *et al.* 2020), and toxicity to aquatic and terrestrial plants (X. Wang *et al.* 2022). Although salinization has historically been confined to arid climates, it is now a global phenomenon encompassing humid regions (Y. Li *et al.* 2022). Major anthropogenic chloride emissions originate from metal manufacturing, coal combustion waste (D. Li *et al.* 2020), textile factories, and food-processing industries. The non-biodegradable and soluble nature of chloride thwarts the conventional treatment techniques. Therefore, the development of efficient chloride removal systems is an urgent priority to prevent the contamination and salinization of limited freshwater reserves.

According to Eq. 2 and Fig. 3, the adsorption of chloride onto the activated carbon surface occurs through physisorption mechanisms, as reported for carotenoids. With decreasing temperature, it was possible to increase the chloride adsorption to 97%. For the pH parameter, the lower the value, the greater the chloride removal efficiency. As the raw effluent has pH values near the lower limit of the investigated range, it is unnecessary to adjust the pH of the effluent for chloride removal by adsorption with activated carbon.

The activated carbon studied has cationic and anionic groups on its surface, allowing the adsorption of either cations or anions depending on the pH of the aqueous medium. Thus, the pH plays a vital role in the adsorption of organic and inorganic contaminants from complex effluents. Based on the presented results, low pH values created more favorable surface conditions for removing both carotenoids and chloride ions.

Other points to consider are the small ionic radii of the chloride anions and their high electronegativity. Their small rays favor chloride penetration through various channels and pores of the adsorbent material. Small coordination rays of chloride promoted a higher distribution of chloride anions across the surface area of the activated carbon. Owing to its higher electronegativity than other chemical species in the effluent, such as carotenoids and even sulfate, its adhesion to anionic functional groups is favored. This was demonstrated by its higher removal rate compared to that of carotenoids and sulfate.

As chloride and carotenoids filled the functional groups, the specific surface area of the adsorbent decreased. We performed measurements using the Brunauer-Emmett-Teller (BET) method on the activated carbon before and after the adsorption process. Activated carbon had a surface area of 411.6253 m^2/g. After the adsorption time, its value decreased by 38%, reaching 254.2262 m^2/g. Therefore, it is clear that the entire surface area was filled with organic and inorganic substances. However, a considerable portion of the pores is expected to be challenging for larger molecules, such as carotenoids or hydrated sulfate anions.

Wang et al. (H. Wang *et al.* 2020) proposed a new method to synthesize phosphorus-doped carbon materials by crosslinking polymerization of *m*-phenylenediamine and phytic acid, followed by carbonization. Phosphorus-doped carbon materials (NPC) showed improved hydrophilicity and electrochemical performance compared to undoped carbon. When tested for capacitive deionization (CDI) desalination, NPC with a 10:1 nitrogen/phosphorus ratio achieved the highest chloride removal capacity of 21.4 mg/g, which was much higher than that of undoped carbon (4.8 mg/g). The improved desalination performance is attributed to the defects induced by phosphorus doping as well as the positively charged phosphorus atoms that can adsorb chloride ions. In each electro-adsorption experiment, the authors used a peristaltic pump to continuously circulate a 30 mL solution containing 500 mg/L of chloride ions between the CDI cell and a beaker at a flow rate of 10 mL/min.

Lv et al. (Lv *et al.* 2006) prepared a calcined layered double hydroxide (CLDH) adsorbent. CLDH was prepared by calcining layered double hydroxides (LDH) containing carbonates at 500°C. The equilibrium adsorption data fit the Langmuir model better than the Freundlich model. The maximum uptake capacity for chloride was 149.5 mg/g, which was close to the stoichiometric capacity. Increasing the temperature, initial chloride concentration, and adsorbent dosage increased the adsorption rate, indicating chemisorption. The amount of adsorbent ranged from 0.5 to 3.0 g/L. The adsorption experiments were conducted at different temperatures ranging from 30 to 70°C. Increasing the temperature significantly increased the chloride adsorption rate. The initial pH of the chloride solution was not controlled or adjusted

during kinetic experiments. The authors stated that no pH control was necessary to prevent contamination by foreign anions that could affect chloride uptake. For the kinetic experiments, NaCl was dissolved in water to prepare 2 L chloride solutions with concentrations ranging from 20 to 2000 mg/L.

4.5. Sulfate removal

While sulfates occur naturally in small, benign concentrations in water systems, elevated levels can impart undesirable qualities. High sulfate concentrations contribute to a sour taste in drinking water and promote pipeline scaling. Concentrations exceeding 500-750 mg/L have laxative effects and cause dehydration and gastrointestinal distress in humans (Chatla *et al.* 2023). Sulfate concentration limits have been established in Brazil to preserve freshwater quality. Brazilian law mandates that total sulfate levels remain below 250 mg/L in potable water (Silva, 2005).

Chemical precipitation is the predominant method for treating sulfate-laden wastewater effluents, which tend to have high sulfate concentrations (Chatla *et al.* 2023). The affordability and straightforward operation of this technique make it the most widely utilized sulfate removal process. The popularity of chemical precipitation stems from its cost-effectiveness and simple implementation for the desulfurization of high-strength wastewater. Despite these advantages, the chemical precipitation of sulfate involves the use of barium. Through practical experience, we know that the excessive use of reagents by operators of effluent treatment plants is common. Consequently, a new contaminant is introduced into the treated effluent. The main cause of acute barium poisoning is the consumption of soluble barium compounds, such as $BaCl_2$, which leads to gastroenteritis (characterized by vomiting, diarrhea, and abdominal pain), low potassium levels (hypokalemia), high blood pressure (hypertension), irregular heartbeats (cardiac arrhythmia), and paralysis of skeletal muscles (Su *et al.* 2020). The smallest lethal acute oral dose of $BaCl_2$ is 11.4 mg/kg (Choudhury & Cary, 2001) body weight, and even a dose as minor as 5.8 mg/kg body weight can result in paresthesia, flaccid paralysis, and muscle weakness (Choudhury & Cary, 2001).

According to our understanding, the development of an adsorption process for sulfate removal would be more appropriate. In addition, the adsorption process is simpler to execute, requiring only exchange of the adsorption column when it becomes saturated. However, the adsorbent material studied was not efficient in removing sulfate anions. It is not possible to obtain a mathematical model with reproducible results. Sulfate ions are larger than chloride ions and have lower electronegativity. Thus, the competitiveness of the adsorption sites is favorable for chloride ions. Furthermore, it is possible to observe the effect of the matrix (effluent) on analytical determinations and adsorption tests that exerted a strong influence on the results obtained. Because the complexity of the sample matrix and the high content of dissolved ions made it practically impossible to determine the adsorption behavior of the species in isolation. In this sense, the proposition of mathematical models that allow explaining the data can be an option to isotherm models that require greater experimental control conditions in order to understand the mechanisms of action.

Hong et al. (Hong *et al.* 2017) investigated three types of activated carbon for removing sulfate from water-bituminous coal-based (UC), hardwood-based (RGC), and oak wood-based (Gran C). RGC had the highest surface area (1101 m^2/g), along with the largest micropore volume (0.339 cm^3/g) and mesopore volume (0.678 cm^3/g). The activated carbons were modified by depositing polypyrrole, which significantly increased their nitrogen content and positively charged surface area. This enhanced the adsorption capacity for negatively charged sulfate ions. Among the polypyrrole-modified carbons, RGC exhibited the highest sulfate adsorption capacity. At lower initial sulfate concentrations of 10 mg/L and 50 mg/L, RGC-polypyrrole achieved uptake of 5.1 mg/g and 20.2 mg/g, respectively. With higher initial sulfate concentrations of 100 mg/L and 250 mg/L, the adsorption capacities increased to 35.5 mg/g and 44.7 mg/g, respectively. Kinetic experiments conducted at room temperature (approximately 25°C) showed that the adsorption equilibrium was attained within 24 h. The effect of temperature was studied by generating adsorption isotherms at 15°C and 35°C. The adsorption capacity increased with increasing temperature, indicating an endothermic process. In summary, polypyrrole-modified RGC were identified as superior adsorbents for sulfate removal, owing to their high surface area and pore volume. It achieved an excellent uptake capacity at higher temperatures.

4.6. FTIR analyses

Infrared spectroscopy provides essential structural information by detecting the vibrations of chemical bonds and functional groups when exposed to IR radiation. Each bond and group vibrate at characteristic frequencies, producing a unique IR spectrum that can be used to elucidate the composition and structure of a material. We aimed to identify specific functional groups in activated carbon samples that are capable of adsorbing pollutants. Fig. 1 displays the IR spectra of activated carbon before (blue spectrum) and after (orange spectrum) the adsorption process. In the spectra, a broad absorption band at 3446 cm^{-1} arises from the —OH stretching of the hydroxyl groups, likely carboxylic acids. The bands at 2978, 2917, and 2849 cm^{-1} represent aliphatic C—H stretches. The peak at 1633 cm^{-1} indicates C=O stretching from ketones, aldehydes, lactones, or carboxylates. This peak may also contain contributions from C=C stretches of alkenes and aromatics. The band at 1384 cm^{-1} originates from the alkyl C—H bending of the methyl groups. The 1086 cm^{-1} peak signifies C—O stretching of aliphatic ethers and alcohols. Finally, bands at 793, 778, and 694 cm^{-1} result from aromatic C—H bonds, indicating adjacent hydrogens on the aromatic rings. There was little difference between the FTIR spectra of raw activated carbon and carbon after the adsorption of compounds from the effluent. More intense bands were obtained at

1633 and 1384 cm^{-1}, probably because of the adsorption of carotenoids with the C=O groups of carboxylic groups.

5. Conclusions

A regression model for norbixin adsorption by activated carbon was successfully obtained. ANOVA analysis revealed that among the parameters studied (temperature, pH, adsorbent mass, and their interactions) linear temperature, linear pH, and temperature × pH interactions are the main terms of the model. The process showed better results under strongly acidic conditions and lower temperatures. Overall, a simple, robust, and reproducible process was developed to remove over 90% of carotenoids from the effluent in a short-time process. These results highlight the potential of activated carbon adsorption as a feasible method for treating food industry effluents containing high load of carotenoids and salts.

The mathematical models obtained by analysis of variance represent (and with low error) the adsorption processes of carotenoids and chloride on activated carbon. However, the traditional Langmuir and Freundlich isotherm models do not represent our adsorption process. Hypotheses that support isotherm models such as pore homogeneity, monolayer formation, constant internal diffusion are not satisfied.

Funding

This research was funded by the São Paulo Research Foundation (FAPESP), Grants 2018/05698-0 (Regular Research Grant) and 2018/17913-2 (Multi-user Equipment) and by the Federal Institute of Education, Science, and Technology of São Paulo (IFSP), Dean of Research funding.

Acknowledgments

We thank senior researcher Dr. Paulo Roberto Nogueira Carvalho (Food Technology Institute, ITAL, Campinas, São Paulo, Brazil) for his valuable contribution to the world of annatto.

References

Alexander Zengeya, M., Ge, D., Li, X., Zhu, N., Zhou, P., Xie, P., & Huang, S. (2024). Porous carbon endows mayenite with high activity to achieve closed-loop removal of chloride ions from desulfurization wastewater. *Chemical Engineering Journal*, *490*, 151834. https://doi.org/10.1016/j.cej.2024.151834

Boguniewicz-Zablocka, J., Klosok-Bazan, I., Callegari, A., & Capodaglio, A. G. (2020). Snack-food industry effluent pre-treatment for annatto dye and yeast removal: Process improvement for effectiveness and sustainability. *Journal of Cleaner Production*, *277*, 124117. https://doi.org/10.1016/j.jclepro.2020.124117

Bouazizi, N., Vieillard, J., Samir, B., & Le Derf, F. (2022). Advances in Amine-Surface Functionalization of Inorganic Adsorbents for Water Treatment and Antimicrobial Activities: A Review. *Polymers*, *14*(3), 378. https://doi.org/10.3390/polym14030378

Carvalho, P. R. N. (2020). *Urucum: A Seed with the History of Brazil* (1st ed.). Evidência.BR.

Chatla, A., Almanassra, I. W., Abushawish, A., Laoui, T., Alawadhi, H., Atieh, M. A., & Ghaffour, N. (2023). Sulphate removal from aqueous solutions: State-of-the-art technologies and future research trends. *Desalination*, *558*, 116615. https://doi.org/10.1016/j.desal.2023.116615

Choudhury, H., & Cary, R. (2001). *Barium and Barium Compounds* (Concise International Chemical Assessment Document 33; p. 53). World Health Organization. https://apps.who.int/iris/bitstream/handle/10665/42398/9241530332.pdf

Coelho Dos Santos, D., Silva Barboza, A. D., Ribeiro, J. S., Rodrigues Junior, S. A., Campos, Â. D., & Lund, R. G. (2022). Bixa orellana L. (Achiote, Annatto) as an antimicrobial agent: A scoping review of its efficiency and technological prospecting. *Journal of Ethnopharmacology*, *287*, 114961. https://doi.org/10.1016/j.jep.2021.114961

D19 Committee. (n.d.-a). *Standard Test Method for Total Nitrogen, and Total Kjeldahl Nitrogen (TKN) by Calculation, in Water by High Temperature Catalytic Combustion and Chemiluminescence Detection*. ASTM International. https://doi.org/10.1520/D8083-16

D19 Committee. (n.d.-b). *Test Method for Total Carbon and Organic Carbon in Water by High Temperature Catalytic Combustion and Infrared Detection*. ASTM International. https://doi.org/10.1520/D7573-18AE01

Dey, S., Ganugula, T. N. V., Padavala, S. S. A. B., & Akula, V. P. M. (2024). An experimental study on the parthenium biosorbents for removals of chlorides and hardness from contaminated water. *Energy Nexus*, *15*, 100309. https://doi.org/10.1016/j.nexus.2024.100309

Florence, T. M., & Farrar, Y. J. (1971). Spectrophotometric determination of chloride at the parts-per-billion level by the mercury(II) thiocyanate method. *Analytica Chimica Acta*, *54*(2), 373–377. https://doi.org/10.1016/S0003-2670(01)82142-5

Gama, B. M. V. D., Selvasembian, R., Giannakoudakis, D. A., Triantafyllidis, K. S., McKay, G., & Meili, L. (2022). Layered Double Hydroxides as Rising-Star Adsorbents for Water Purification: A Brief Discussion. *Molecules*, *27*(15), 4900. https://doi.org/10.3390/molecules27154900

Guo, J., Zhou, Z., Ming, Q., Huang, Z., Zhu, J., Zhang, S., Xu, J., Xi, J., Zhao, Q., & Zhao, X. (2022). Recovering precipitates from dechlorination process of saline wastewater as poly aluminum chloride. *Chemical Engineering Journal*, *427*, 131612. https://doi.org/10.1016/j.cej.2021.131612

Hirko, B., & Getu, A. (2022). Bixa Orellana (Annatto Bixa): A Review on Use, Structure, Extraction Methods and Analysis. *Journal of Agronomy, Technology and Engineering Management*, *5*(1), 687–696.

Hong, S., Cannon, F. S., Hou, P., Byrne, T., & Nieto-Delgado, C. (2017). Adsorptive removal of sulfate from acid mine drainage by polypyrrole modified activated carbons: Effects of polypyrrole deposition protocols and activated carbon source. *Chemosphere*, *184*, 429–437. https://doi.org/10.1016/j.chemosphere.2017.06.019

Igansi, A. V., Engelmann, J., Lütke, S. F., Porto, F. B., Pinto, L. A. A., & Cadaval, T. R. S. (2019). Isotherms, kinetics, and thermodynamic studies for adsorption of pigments and oxidation products in oil bleaching from catfish waste. *Chemical Engineering Communications*, *206*(11), 1399–1413. https://doi.org/10.1080/00986445.2018.1539965

Kalra, R., Gaur, S., & Goel, M. (2021). Microalgae bioremediation: A perspective towards wastewater treatment along with industrial carotenoids production.

Journal of Water Process Engineering, *40*, 101794. https://doi.org/10.1016/j.jwpe.2020.101794

Kapoor, L., & Ramamoorthy, S. (2021). Strategies to meet the global demand for natural food colorant bixin: A multidisciplinary approach. *Journal of Biotechnology*, *338*, 40–51. https://doi.org/10.1016/j.jbiotec.2021.07.007

Lau, S. Y., Phuan, S. L., Danquah, M. K., & Acquah, C. (2019). Sustainable palm oil refining using pelletized and surface-modified oil palm boiler ash (OPBA) biosorbent. *Journal of Cleaner Production*, *230*, 527–535. https://doi.org/10.1016/j.jclepro.2019.04.390

Li, D., Liu, J., Wang, S., & Cheng, J. (2020). Study on coal water slurries prepared from coal chemical wastewater and their industrial application. *Applied Energy*, *268*, 114976. https://doi.org/10.1016/j.apenergy.2020.114976

Li, Y., Yang, Z., Yang, K., Wei, J., Li, Z., Ma, C., Yang, X., Wang, T., Zeng, G., Yu, G., Yu, Z., & Zhang, C. (2022). Removal of chloride from water and wastewater: Removal mechanisms and recent trends. *Science of The Total Environment*, *821*, 153174. https://doi.org/10.1016/j.scitotenv.2022.153174

Li, Z.-C., Li, W., Wang, R., Wang, D.-X., Tang, A.-N., Wang, X.-P., Gao, X.-P., Zhao, G.-M., & Kong, D.-M. (2023). Lignin-based covalent organic polymers with improved crystallinity for non-targeted analysis of chemical hazards in food samples. *Journal of Hazardous Materials*, *448*, 130821. https://doi.org/10.1016/j.jhazmat.2023.130821

Lv, L., He, J., Wei, M., Evans, D. G., & Duan, X. (2006). Uptake of chloride ion from aqueous solution by calcined layered double hydroxides: Equilibrium and kinetic studies. *Water Research*, *40*(4), 735–743. https://doi.org/10.1016/j.watres.2005.11.043

Moosaei, R., Sabbaghi, S., Sadegh Jafari Zadegan, M., Rasouli, K., Ghaedi, S., & Rajabi, H. (2024). Silver nanoparticles modified titanium carbide MXene composite for RSM-CCD optimised chloride removal from water. *Journal of Molecular Liquids*, *399*, 124480. https://doi.org/10.1016/j.molliq.2024.124480

Pavithra, K. G., P., S. K., V., J., & P., S. R. (2019). Removal of colorants from wastewater: A review on sources and treatment strategies. *Journal of Industrial and Engineering Chemistry*, *75*, 1–19. https://doi.org/10.1016/j.jiec.2019.02.011

Pohndorf, R. S., Cadaval, T. R. S., & Pinto, L. A. A. (2016). Kinetics and thermodynamics adsorption of carotenoids and chlorophylls in rice bran oil bleaching. *Journal of Food Engineering*, *185*, 9–16. https://doi.org/10.1016/j.jfoodeng.2016.03.028

Rathi, B. S., & Kumar, P. S. (2021). Application of adsorption process for effective removal of emerging contaminants from water and wastewater. *Environmental Pollution*, *280*, 116995. https://doi.org/10.1016/j.envpol.2021.116995

Reith, J. F., & Gielen, J. W. (1971). Properties of Bixin and Norbixinand the Composition of Annatto Extracts. *Journal of Food Science*, *36*(6), 861–864. https://doi.org/10.1111/j.1365-2621.1971.tb15545.x

Salazar, R. F. S., Guerra, M. B. B., Pereira-Filho, E. R., & Nóbrega, J. A. (2011). Performance evaluation of collision–reaction interface and internal standardization in quadrupole ICP-MS measurements. *Talanta*, *86*, 241–247. https://doi.org/10.1016/j.talanta.2011.09.009

Samanta, A. K., & Singhee, D. (2023). Sources, Application, and Analysis of Natural Colorants: An Indian Perspective. In C. Stevens, T. Bechtold, A. Manian, & T. Pham (Eds.), *Handbook of Natural Colorants* (1st ed., pp. 103–159). Wiley. https://doi.org/10.1002/9781119811749.ch8

Sarani, P., Sabbaghi, S., Rasouli, K., Mirbagheri, N. S., & Rasouli, J. (2024). Optimization of chloride ion removal from drinking water using graphene oxide modified with AgNO3 via CCD-based RSM method. *Inorganic Chemistry Communications*, *160*, 111930. https://doi.org/10.1016/j.inoche.2023.111930

Silva, M. (2005). *CONAMA Resolution n. 357/2005*. https://www2.cprh.pe.gov.br/wp-content/uploads/2021/02/resol-conama357.pdf

Singh, K., Dave, H., Prasad, B., Kumari, M., Dubey, D., Rai, A. K., Ravi, R., Manjhi, J., Sillanpää, M., & Prasad, K. S. (2024). nFeO decorated wood biochar as an adsorbent for aqueous Cr(VI) ions: Hyphenated, coagulation-column treatment of tannery effluent. *Journal of Water Process Engineering*, *59*, 105084. https://doi.org/10.1016/j.jwpe.2024.105084

Strieder, M. M., Pinheiro, C. P., Borba, V. S., Pohndorf, R. S., Cadaval, T. R. S., & Pinto, L. A. A. (2017). Bleaching optimization and winterization step evaluation in the refinement of rice bran oil. *Separation and Purification Technology*, *175*, 72–78. https://doi.org/10.1016/j.seppur.2016.11.026

Su, J.-F., Le, D.-P., Liu, C.-H., Lin, J.-D., & Xiao, X.-J. (2020). Critical care management of patients with barium poisoning: A case series. *Chinese Medical Journal*, *6*, 724–725. https://doi.org/10.1097/CM9.0000000000000672

Sun, S., Guo, N., & Fu, Y. (2016). Adsorption of β-carotene on modified magnesium silicate. *Russian Journal of Physical Chemistry A*, *90*(2), 443–450. https://doi.org/10.1134/S0036024415130348

SW-846 Test Method 9038: Sulfate (Turbidimetric) (METHOD 9038). (1986).

Valério, M. A., Ramos, M. I. L., Braga Neto, J. A., & Macedo, M. L. R. (2015). Annatto seed residue (Bixa orellana L.): Nutritional quality. *Food Science and Technology (Campinas)*, *35*(2), 326–330. https://doi.org/10.1590/1678-457X.6539

Wang, H., Yuan, T., Huang, L., He, Y., Wu, B., Hou, L., Liao, Q., & Yang, W. (2020). Enhanced chloride removal of phosphorus doping in carbon material for capacitive deionization: Experimental measurement and theoretical calculation. *Science of The Total Environment*, *720*, 137637. https://doi.org/10.1016/j.scitotenv.2020.137637

Wang, X., Gao, K., Ma, J., Liu, F., Wang, X., Li, D., & Yang, M. (2022). Analysis of the chloride ion removal mechanism from simulated wastewater by discarded vitamin tablets. *Water Science and Technology*, *86*(10), 2483–2494. https://doi.org/10.2166/wst.2022.355

Zhang, L., Lv, P., He, Y., Li, S., Chen, K., & Yin, S. (2020). Purification of chlorine-containing wastewater using solvent extraction. *Journal of Cleaner Production*, *273*, 122863. https://doi.org/10.1016/j.jclepro.2020.122863

Supplementary material

Statistical analysis of adsorption process

Carotenoids adsorption

Table S1. Analysis of variance for carotenoids removal fit regression model: (a) complete model; (b) refined model. Degrees of Freedom (DF). Adjusted Sums of Squares (Adj. SS) for different model components. Adjusted Mean Squares of the errors (Adj. MS, or variance s2). 95% confidence level (α = 0.05).

			(a)						(b)		
Source	**DF**	**Adj. SS**	**Adj. MS**	**F-value**	**P-value**	**Source**	**DF**	**Adj. SS**	**Adj. MS**	**F-value**	**P-value**
T	1	267.1516	267.1516	56.04720	0.001702	T	1	267.1516	267.1516	41.25828	0.000673
m_{ads}	1	1.0878	1.0878	0.22822	0.657782	pH	1	201.1015	201.1015	31.05766	0.001416
pH	1	201.1015	201.1015	42.19019	0.002898	T*m_{ads}	1	55.7040	55.7040	8.60280	0.026183
T*m_{ads}	1	55.7040	55.7040	11.68645	0.026816	T*pH	1	381.8466	381.8466	58.97152	0.000255
T*pH	1	381.8466	381.8466	80.10969	0.000862	Error	6	38.8506	6.4751		
m_{ads}*pH	1	18.6966	18.6966	3.92246	0.118731	Total	10	944.6544			
Error	4	19.0662	4.7665								
Total	10	944.6544									

Table S2. Analysis of variance for chloride removal fit regression model: (a) complete model; (b) refined model. Degrees of Freedom (DF). Adjusted Sums of Squares (Adj. SS) for different model components. Adjusted Mean Squares of the errors (Adj. MS, or variance s2). 95% confidence level (α = 0.05).

			(a)						(b)		
Source	**DF**	**Adj. SS**	**Adj. MS**	**F-value**	**P-value**	**Source**	**DF**	**Adj. SS**	**Adj. MS**	**F-value**	**P-value**
T	1	231.663	231.663	4.22	0.109	m_{ads}	1	589.103	589.103	8.82	0.021
m_{ads}	1	589.103	589.103	10.74	0.031	T*m_{ads}	1	1397.354	1397.354	20.93	0.003
pH	1	5.865	5.865	0.11	0.760	m_{ads}*pH	1	604.303	604.303	9.05	0.020
T*m_{ads}	1	1397.354	1397.354	25.47	0.007	Error	7	467.289	66.756		
T*pH	1	10.283	10.283	0.19	0.687	Total	10	3058.049			
m_{ads}*pH	1	604.303	604.303	11.01	0.029						
Error	4	219.478	54.869								
Total	10	3058.049									

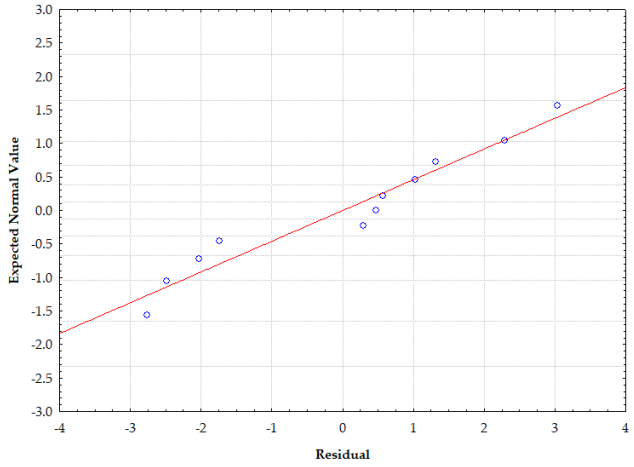

Figure S1. Normal probability plot of residuals from the carotenoids adsorption (%) process.

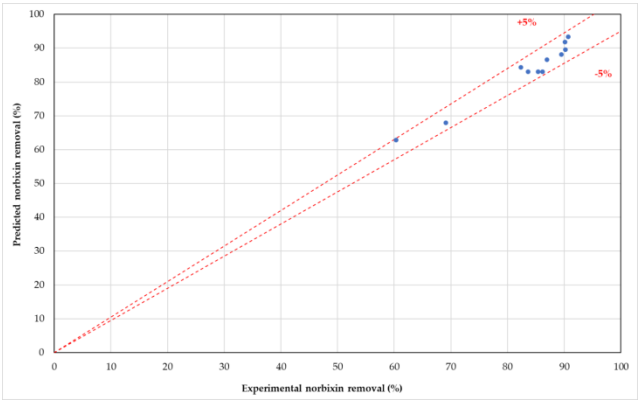

Figure S2. Predicted *versus* experimental values of carotenoids removal (%).

Chloride adsorption

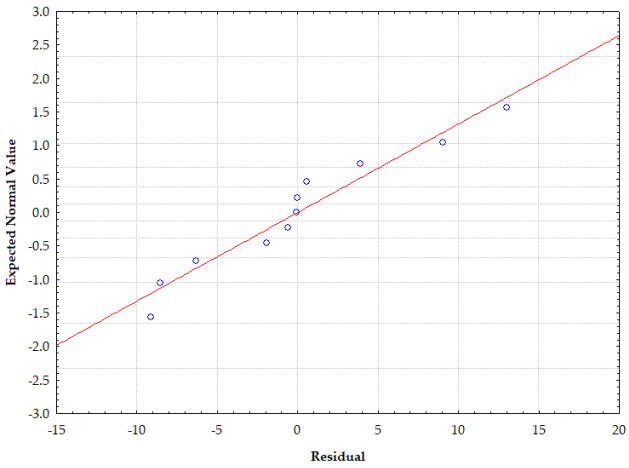

Figure S3. Normal probability plot of residuals from the chloride adsorption (%) process.

Langmuir model (carotenoids)

The Eq. (3) shows the adsorption model by Langmuir isotherms. The Eq. (4) shows the linear form of the Langmuir model.

$$q_e = \frac{K_L\ C_e}{1+K_L\ C_e} \quad (3)$$

Langmuir equation as a linear model:

$$\frac{1}{q_e} = \frac{1}{q_m} + \frac{1}{q_m K_L}\frac{1}{C_e} \quad (4)$$

Q_m: maximum adsorption capacity of the monolayer

K_L= kinetic equilibrium between adsorption and desorption

q_e= equilibrium fractional occupancy of adsorption sites

C_0= initial concentration of solute

C_e= concentration of solute in equilibrium with the surface

Table S3. Experimental data on the adsorption of carotenoids by activated carbon. Example to illustrate the inapplicability of the Langmuir isotherm model with the effluent from the annatto dye industry.

Exp.	Dilution factor	C_0 (mg/L)	C_e (mg/L)	q_e (mg/g)
1	10x	524,60	3,156	13,0361
2	20x	260,37	2,7615	6,4402125
3	30x	175,158	3,4321	4,2931475
4	40x	131,368	2,9074	3,211515
5	50x	104,937	3,0376	2,547485
6	75x	69,8265	1,2229	1,71509
7	100x	52,4685	1,499	1,2742375

Table S4. Experimental data on the adsorption of carotenoids by activated carbon. Example to illustrate the inapplicability of the Freundlich isotherm model with the effluent from the annatto dye industry.

Exp.	Dilution factor	log C_e	log q_e
1	10x	0,499136995	1,115147683
2	20x	0,441145048	0,808900197
3	30x	0,535559933	0,63277581
4	40x	0,463504786	0,506709955
5	50x	0,482530584	0,406111635
6	75x	0,087390945	0,234286915
7	100x	0,175801633	0,105250382

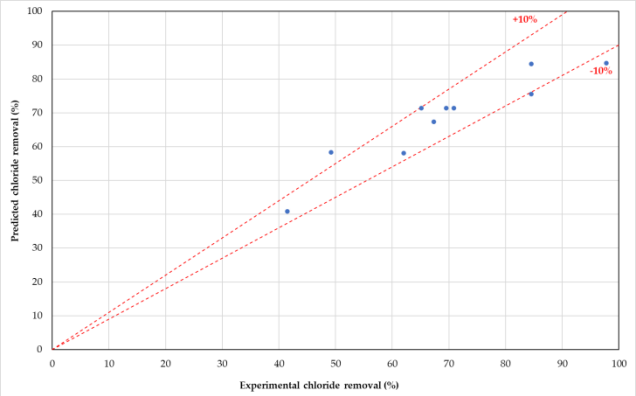

Figure S4. Predicted *versus* experimental values of chloride removal (%).

Freundlich Model (carotenoids)

The Eq. (5) shows the adsorption model by Freundlich isotherm. The Eq. (6) shows the linear form of the Freundlich model.

$$q_e = K_F C_e^{1/n} \quad (5)$$

Freundlich equation as a linear model:

$$ln(q_e) = ln(K_F) + \frac{1}{n} C_e \quad (6)$$

q_e: equilibrium fractional occupancy of adsorption sites

K_F: Freundlich constant (mg/g)

C_e: concentration of solute in equilibrium with the surface

n: empirical parameter

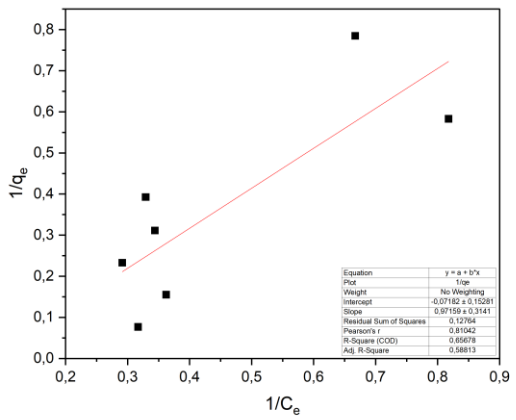

Figure S5. Experimental data on the adsorption of carotenoids by activated carbon. Example to illustrate the inapplicability of the Langmuir isotherm model with the effluent from the annatto dye industry.

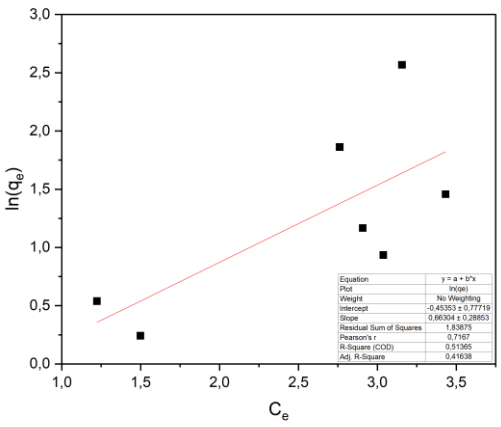

Figure S6. Experimental data on the adsorption of carotenoids by activated carbon. Example to illustrate the inapplicability of the Freundlich isotherm model with the effluent from the annatto dye industry.